EFFECT OF ATMOSPHERIC CORRECTION ALGORITHM ON LANDSAT-8 AND SENTINEL-2 CLASSIFICATION ACCURACY IN PADDY FIELD AREA

Fadila Muchsin[1], Kuncoro Adi Pradono[2], Indah Prasasti[1], Dianovita[1], Kurnia Ulfa[1], Kiki Winda Veronica[1], Dandy Aditya Novresiandi[1], Andi Ibrahim[1]

[1] Research Center for Remote Sensing, National Research and Innovation Agency (BRIN)
[2] Directorate of Laboratory Management, Research Facilities, and Science and Technology Park, National Research and Innovation Agency (BRIN)

e-mail: kurnia.ulfa@brin.go.id

Received: 19.01.2023; Revised: 31.05.2023; Approved: 31.05.2023

Abstract. Landsat-8 and Sentinel-2 satellite imageries are widely used for various remote sensing applications because they are easy to access and free to download. A precise atmospheric correction is necessary to be applied to the optical satellite imageries so that the derived information becomes more accurate and reliable. In this study, the performance of atmospheric correction algorithms (i.e., 6S, FLAASH, DOS, LaSRC, and Sen2Cor) was evaluated by comparing the object's spectral response, vegetation index, and classification accuracy in the paddy field area before and after the implementation of atmospheric correction. Overall, the results show that each algorithm has varying accuracy. Nevertheless, all atmospheric correction algorithms can improve the classification accuracy, whereby those derived by the 6S and FLAASH yielded the highest accuracy.

Keywords: *atmospheric correction, Landsat-8, Sentinel-2, classification accuracy*

1 INTRODUCTION

Landsat 8 Surface Reflectance (SR) Science Products are generated from Land Surface Reflectance Code (LaSRC) derived from NASA LaSRC. The original LaSRC algorithm was developed by Eric Vermote, National Aeronautics and Space Administration (NASA) Goddard Space Flight Center (GSFC) and was modified by the USGS Earth Resources Observation and Science (EROS) Center. LaSRC generates Top of Atmosphere (TOA) Reflectance and TOA Brightness Temperature (BT) using the calibration parameters from the metadata. Atmospheric correction routines are then applied to Landsat 8 TOA Reflectance data, using auxiliary input data such as water vapor, ozone, and Aerosol Optical Thickness (AOT) retrieved from Moderate Resolution Imaging Spectroradiometer (MODIS), and digital elevation derived from Earth Topography Five Minute Grid (ETOPO5) to generate Surface Reflectance. The result is delivered as the Landsat Surface Reflectance data product which use internal algorithm and can be found on EarthExplorer. The LaSRC algorithm is distinctly different from the algorithm used to process Landsat 4–5 Thematic Mapper (TM) and Landsat 7 Enhanced Thematic Mapper Plus (ETM+) Level 1 (L1) products to Surface Reflectance, known as the Landsat Ecosystem Disturbance Adaptive Processing System (LEDAPS) which was developed by Jeff Masek and the algorithm was the Second Simulation of the Satellite Signal in the Solar Spectrum (6S). Collection 2 Landsat 8 L2SP are generated at 30-meter spatial resolution on a Universal Transverse Mercator (UTM) or Polar Stereographic (PS) mapping grid as reflecance products. All packages include Extensible Markup Language (XML) and JavaScript Object Notation (JSON)-based metadata. Collection 2 Landsat 8 L2SP are delivered in files named with the ProductID and appended with "_SR_"(Surface Reflectance) or "_ST_" followed by the

band designation. The default file format is COG (USGS, 2022).

Sentinel-2 Products used in this research was Level-1C product provides orthorectified image and the algorithm Top-Of-Atmosphere (TOA) to produce reflectance, with sub-pixel multispectral registration. Cloud and land/water masks are included in the product. This is an orthoimage product i.e., a map projection of the acquired image using a system DEM to correct ground geometric distortions. Pixel radiometric measurements are provided in Top-Of-Atmosphere (TOA) reflectances with all parameters to transform them into radiances. Level-1C products are resampled with a constant GSD (Ground Sampling Distance) of 10m, 20m and 60m according to the native resolution of the different spectral bands. In addition, the Level-1C User Product embeds always a GRANULE (tile) level an elementary set of meteorological and atmospheric datasets extracted and resampled from European Centre for Medium-range Weather Forecasts (ECMWF). forecast output and relevant to down-stream processing (i.e atmospheric corrections). The ECMWF auxiliary data embedded in the Level-1C at Tile level includes Total column ozone (TCO3), Total column water vapour (TCWV), Mean Sea level pressure, 10-meter u/v wind components and Relative Humidity (at surface pressure). Resulting from a temporal and spatial interpolation of the raw ECMWF global forecast dataset, this data will be provided as part of the Level-1C auxiliary data resampled and distributed in grid information tiles with the same dimensions as the Level-1C Tiles. Grid points are provided in latitude/longitude using WGS84 reference system (European Space Agency, 2022)

Landsat-8 and Sentinel-2 data enable efficient monitoring of rice plant growth at a field scale with a spatial resolution of up to 10 meters and a temporal resolution of every 5 days. The combination of Landsat-8 and Sentinel-2 data generates high-frequency and high-spatial resolution data for free, making monitoring extremely fast (B. Franch, Vermote, Sobrino, & Fédèle, 2013);(Belen Franch et al., 2021).

Atmospheric correction is an important step in pre-processing satellite data, especially for multitemporal classification and extraction of surface biophysical parameters from optical images. The purpose of atmospheric correction is to remove the influence of the atmosphere on the image so that the surface reflectance value is obtained (Claverie et al., 2018).

Assessment of atmospheric correction on sentinel-2 data was carried out by comparing four methods, namely Sen2cor, MAJA, 6S, and ICOR. The results found that the need for an accurate atmospheric correction is an essential pre-processing step for a large number of remote sensing application, especially multitemporal studies (Sola et al., 2018). An atmospheric correction method based on the solar radiation transfer model has been developed. This shows that the algorithm allows one to significantly improve the image quality of objects in the earth's surface and adequately reproduce its spectral reflectance characteristics (Lisenko, 2018).

Atmospheric correction of the Landsat-7 image for the Jakarta area has been carried out using the 6S, LEDAPS and FLAASH correction models and compared with the TOA reflectance image. The results show a decrease in the object's spectral response after atmospheric correction to the TOA reflectance so that it can improve the spectral pattern of the object following the object's spectral pattern in the image Landsat especially in the blue, green, and red channels. Furthermore, there is a tendency of the same percentage increase and decrease in the FLAASH and 6S methods for all objects and the average value of NDVI (Fadila Muchsin, Fibriawati, & Pradhono, 2018). Comparison of atmospheric correction between FLAASH and 6S has been studied over paddy fields in the Subang area, and the results show that the 6S model has better accuracy for the spectral response of the rice growth phase compared to the FLAASH model (F. Muchsin et al., 2019).

Evaluation of the atmospheric correction algorithm for Sentinel-2 over rice fields have been carried out in the Sukabumi district using Sen2Cor

algorithm (Ulfa et al., 2020), and Cianjur and Klaten regency using DOS and 6S atmospheres correction methods (F. Muchsin, Supriyatna, Harmoko, & Prasasti, 2022). The results showed that the 6S model had better accuracy for the spectral response of the rice plant phase compared to the DOS model.

The aim of this study was to evaluate surface reflectance of five atmospheric correction algorithms (6S, FLAASH, DOS, LaSRC and Sen2cor) and compare classification accuracy after using atmospheric correction in the rice fields of Kupang district. The previous study used Landsat-8 data, while in this study other than Landsat-8, Sentinel-2 data was used. The use of Sentinel-2 data which is acquired every 5 days is expected to complement the data from Landsat-8 which is acquired repeatedly every 10 days. 6S, FLAASH, and DOS methods will be used on both data. Meanwhile, the LaSRC and Sen2cor methods are only used on Landsat-8 and Sentinel-2, respectively. The comparison of the results was briefly described in this paper.

2 MATERIALS AND METHODOLOGY

2.1 Location and Data

The Landsat-8 and Sentinel-2 data used in this study are shown in Table 1. They are multispectral data (visible and NIR band) with a spatial resolution of 10 meters and 30 meters, respectively. The study location were paddy fields in the Kupang Regency, East Nusa Tenggara province (Figure 2-1).

Table 2-1: Satellite data used in this study

Satellite Data	Scene ID	Acquisition Date
Landsat-8	LC08_L1TP_111067_20210428_20210507_02_T1	2021-04-28
Sentinel-2	L1C_T51LWJ_A021636_20210428T020440	2021-04-28

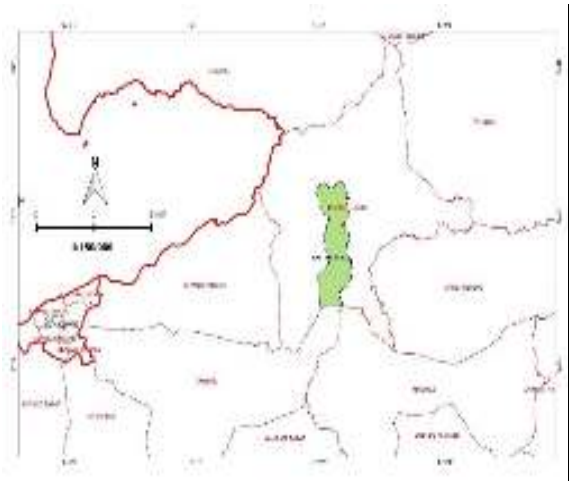

Figure 2-1: Study area location (green polygon)

Figure 2-2: (a) Scene of Landsat-8 image and (b) Scene of Sentinel-2 image

Kupang Regency is a regency in the province of East Nusa Tenggara, Indonesia. The capital of Kupang Regency is located in Oelamasi. Kupang Regency is a district with a hilly topography and part of it is a lowland area spread over the coastal area. The land surface in Kupang

Regency is generally hilly and mountainous and partly consists of lowlands with a slope of up to 45º. Topographically, Kupang Regency generally has a tropical and dry climate which also tends to be influenced by wind and is categorized as a semi-arid area due to relatively low rainfall and vegetation conditions which are dominated by savanna and steppes. This district also has a dry climate type D4 and E4, with climate conditions like this the season is very short, namely 3-5 months, while the dry season is 7-8 months. The short rainy season only occurs from December to March. Figure 2 shows the scenes of Landsat-8 and Sentinel-2 images according to the table 2-1 respectively.

2.2 Atmospheric Correction Algorithm

2.2.1 6S

The 6S (Second Simulation of Satellite Signal method in the Solar Spectrum) algorithm was developed by Vermote et al. based on the 5S model. It considers the atmospheric effects of the entire radiative transfer process and can better eliminate the influence of Rayleigh scattering and aerosols, which has been widely used in applications (Vermote & Kotchenova, 2008).

2.2.2 FLAASH

The FLAASH (Fast Line-of-sight Atmospheric Analysis of Spectral Hypercubus) algorithm is a software package developed by the Air Force Research Laboratory, Space Vehicles Directorate (AFRLiVS), Hanscom AFB and Spectral Sciences, Inc. (SSI) to support the analyses of visible-to-shortwave infra- red (Vis - SWIR) hyperspectral and multispectral imaging sensors.

2.2.3 DOS

DOS is a widely atmospheric correction method. It is based on the assumption that if dark objects, such as dense vegetation or deep water, are in complete shadow and have zero reflectance, the value registered by the sensor must be only due to atmospheric scattering (Chavez, 1996).

2.2.4 LaSRC

LaSRC is an algorithm that was developed by USGS to produce surface reflectance product derive from Landsat data. This product can be downloaded freely from: https://earthexplorer.usgs.gov/.

2.2.5 Sen2Cor

Sen2Cor is an algorithm developed by ESA specifically for Sentinel-2 satellites, and the code is freely available as a SNAP (Sentinel Application Platform) plugin. Users can also obtain Sentinel-2 products corrected with the Sen2Cor algorithm by downloading them directly from: https://scihub.copernicus.eu/dhus/#/home.

2.3 Processing algorithm

Initially, the precision and terrain correction product (L1TP processing level) of Landsat-8 data and the radiometric and geometric correction product (Level-1C processing level) of Sentinel-2 data of the study area were downloaded from the Earth Explorer and Copernicus Open Access Hub, respectively. Afterward, each image was applied to each atmospheric correction procedure specific to each algorithm (i.e., the 6S, FLAASH, and DOS algorithms) to obtain its atmospherically corrected surface reflectance product. Meanwhile, the surface reflectance products applied with LaSRC (Level-2 atmospherically corrected processing level of Landsat-8) and Sen2Cor (Level-2A bottom-of-atmosphere processing level of Sentinel-2) algorithms of the study area were downloaded directly from their associated image provider. This study used these imageries as the input for further image analysis. The algorithm processing can be seen in the figure 3.

2.4 Classification accuracy

After atmospheric correction, the image is classified using a machine learning algorithm, namely Random Forest classification.

RF algorithm is a general term for ensemble learning method which operates using a combination of tree-type classifier in such way that each classifier is generated using random vector which has same distribution for all past random vectors, and it is sampled independently from the values of the input vector. After the creation of the determined number of trees, they vote for the most popular class, so the final output is determined by a majority of the vote.

Random forest (RF) is known to be one of the most efficient classification methods (Ghimire, Rogan, & Miller, 2010). A random forest is a classifier consisting of a collection of tree-structured classifiers {h(x,Θk), k=1, ...} where the {Θ k} are independent identically distributed random vectors and each tree casts a unit vote for the most popular class at input x (Breiman, 2001). RF classification algorithm gives 10% higher accuracy than Support Vector Machine (SVM) algorithm, whereas Gentle and Boost algorithm has 14% accuracy lower than RF classification (Akar & Güngör, 2012).

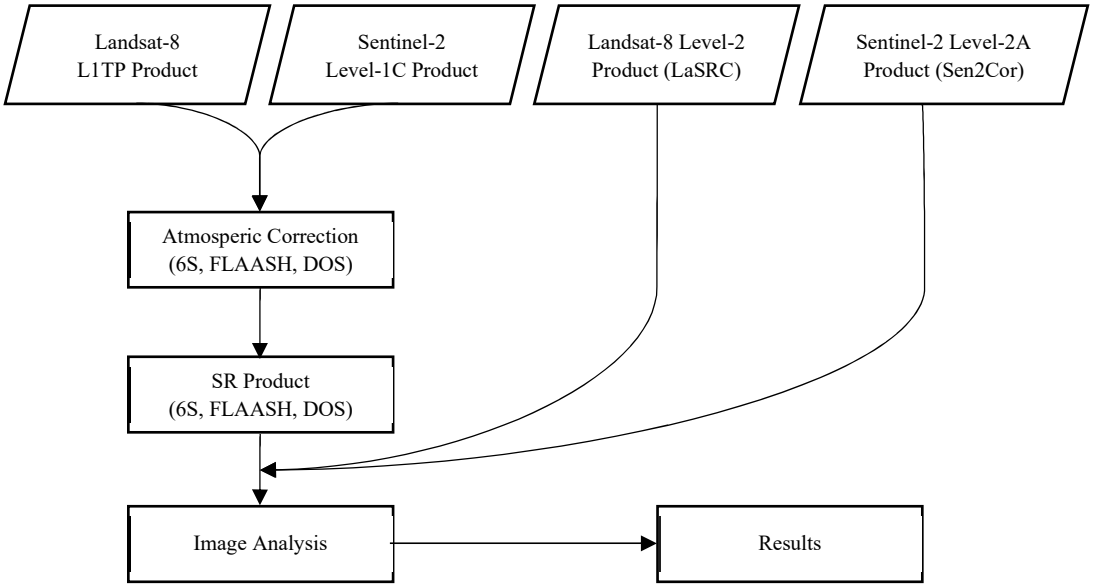

Figure 2-1: Methodological flowchart of the study

3 RESULTS AND DISCUSSION

3.1. Object Spectral Response

The spectral response of a cropland field (10°06'10.8"S 123°48'46.4"E) in the study area for the Landsat-8 image is presented figure 4. All atmospherically corrected images yielded lower reflectance values on red, green, and blue bands compared to the standard L1TP product. Additionally, only that derived by the 6S algorithm generated a higher reflectance value on the near-infrared band compared to the standard L1TP product. The atmospherically corrected image derived by the DOS algorithm resulted in a similar pattern to that of the standard L1TP product. Meanwhile, those produced using LaSRC and FLAASH algorithms have the same pattern of spectral responses. In addition, the atmospherically corrected image generated by 6S algorithms produced the lowest reflectance values on red, green, and blue bands but the highest on the near-infrared band.

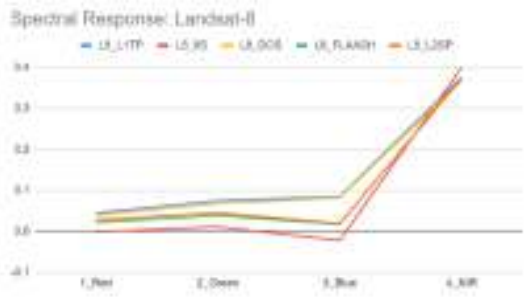

Figure 3-1: Spectral response of Landsat-8 image

For the Sentinel-2 image, the spectral response of the same cropland field in the study area is displayed in figure 3-2. All atmospherically corrected images produced lower reflectance values on red, green, and blue bands compared to the standard L1C product. However, on the near-infrared band, all atmospherically corrected images generated a higher value as compared to the standard L1C product. The DOS algorithm yielded the lowest value on the green band, and the Sen2Cor algorithm generated the lowest value on the red and blue bands. In addition, the highest reflectance value on the near-infrared band is produced by the Sen2Cor algorithm.

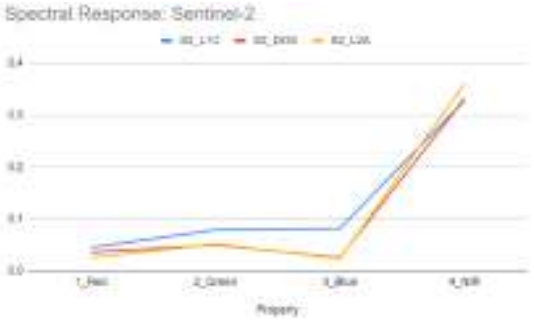

Figure 3-2: Spectral response of Sentinel-2 image

In general, atmosphere correction reduced the reflectance values on the red, green, and blue bands, as shown in both Landsat-8 and Sentinel-2 atmospherically corrected images. As for the near-infrared band, particular algorithms (i.e., the 6S algorithm on the Landsat-8 image; the DOS and Sen2Cor algorithms on the Sentinel-2 image) tend to increase the reflectance values, especially on a selected cropland field in the study area.

3.2 Classification Results

To further understand the influence of atmosphere correction on Landsat-8 and Sentinel-2 images, the atmospherically corrected images were used as input for a land cover classification using the random forest classifier. In this study, four land cover classes were generated, i.e., waterbody, settlements, cropland-1 (defined as cropland areas under vegetated conditions), and cropland-2 (defined as cropland areas under un-vegetated / bare soil conditions). Afterward, accuracy indicators, i.e., Overall Accuracy (OA), Kappa coefficient, Producer's Accuracy (PA), and User's Accuracy (UA), were used to analyze the classification results.

Table 3-1 displayed the result of the accuracy assessment for the land cover classification using the atmospherically corrected Landsat-8 images. The classification result indicated that all images (the standard L1TP and atmospherically corrected images) successfully obtained a very good result in identifying the cropland-1 class as shown in their PA and UA (100% of PA and UA). As for identifying the cropland-2 class, that generated by the LaSRC algorithm yielded the best accuracy (80% of PA and 74.07 of UA). Moreover, the FLAASH algorithm yielded the highest OA and Kappa (86.75% of OA and 0.82 of Kappa) among all Landsat-8 images. The 6S algorithm resulted in the lowest OA and Kappa (71.88% of OA and 0.57 of Kappa) among all Landsat-8 images because it failed to classify the negative reflectance values of waterbody areas generated from the algorithm.

The result of the accuracy assessment for the land cover classification using the atmospherically corrected Sentinel-2 images is presented in table 3-2. The classification result indicated that the DOS algorithm produced the highest PA and UA (100% of PA and UA) in identifying the cropland-1 class.

Table 3-1: Classification results of Landsat-8 image

	OA (%)	Kappa	Waterbody		Settlement		Cropland-1		Cropland-2	
			PA (%)	UA(%)	PA (%)	UA(%)	PA (%)	UA(%)	PA (%)	UA(%)
L8_L1TP	84.71	0.79	100.00	100.00	76.00	73.08	100.00	100.00	72.00	75.00
L8_6S	71.88	0.57	0.00	0.00	52.00	68.42	100.00	100.00	76.00	61.29
L8_DOS	78.82	0.71	100.00	100.00	60.00	65.22	100.00	100.00	68.00	62.96
L8_FLAASH	86.75	0.82	100.00	100.00	84.00	75.00	100.00	100.00	72.00	81.82
L8_L2SP	85.88	0.81	100.00	100.00	72.00	78.26	100.00	100.00	80.00	74.07

Along with that, the Sen2Cor algorithm yielded the highest PA and UA (88% of PA and UA) in identifying the cropland-2 class. Moreover, the Sen2Cor algorithm generated the highest OA and Kappa (91.76% of OA and 0.89 of Kappa) among all Sentinel-2 images. The DOS algorithm resulted in the lowest OA and Kappa (89.41% of OA and 0.85 of Kappa) among all Sentinel-2 images.

Table 3-2: Classification results of Sentinel-2 image

	OA (%)	Kappa	Waterbody		Settlement		Cropland-1		Cropland-2	
			PA (%)	UA(%)	PA (%)	UA(%)	PA (%)	UA(%)	PA (%)	UA(%)
S2_L1C	90.59	0.87	100.00	100.00	84.00	84.00	100.00	96.15	84.00	87.50
S2_DOS	89.41	0.85	100.00	100.00	80.00	83.33	100.00	100.00	84.00	80.77
S2_L2A	91.76	0.89	100.00	100.00	84.00	87.50	100.00	96.15	88.00	88.00

CONCLUSION

Overall, the classification results generated by the Sentinel-2 images outperformed those derived by the Landsat-8 images in this study, which means the greater spatial resolution of an optical image contributes to improving classification accuracy. Besides, the classification results of atmospherically corrected images using particular algorithms (i.e., the LaSRC and FLAASH algorithms on the Landsat-8 image; the Sen2Cor algorithm on the Sentinel-2 image) outperformed those derived by the standard image product (i.e., L1TP of Landsat-8; L1C of Sentinel-2), which means that atmospheric correction also plays an important role in improving classification accuracy so that the provided information from optical satellite imageries becomes more accurate and reliable, especially in studies concerning cropland areas.

ACKNOWLEDGEMENTS

This research was funded by BRIN. The author would like to thank Pusdatin for providing data.

REFERENCES

Akar, Ö., & Güngör, O. (2012). Classification of multispectral images using Random Forest algorithm. *Journal of Geodesy and Geoinformation*, *1*(2), 105–112. https://doi.org/10.9733/jgg.241212.1

Breiman, L. (2001). Random Forest. In *Random Forest* (45th ed., Vol. 45). https://doi.org/10.14569/ijacsa.2016.070603

Chavez, P. S. (1996). Image-based atmospheric corrections - Revisited and improved. *Photogrammetric Engineering and Remote Sensing*, *62*(9), 1025–1036.

Claverie, M., Ju, J., Masek, J. G., Dungan, J. L., Vermote, E. F., Roger, J. C., … Justice, C. (2018). The Harmonized Landsat and Sentinel-2 surface reflectance data set. *Remote Sensing of Environment*, *219*(August 2017), 145–161. https://doi.org/10.1016/j.rse.2018.09.002

European Space Agency. (2022). *Sentinel-2 Products Specification Document (PSD)*.

Franch, B., Vermote, E. F., Sobrino, J. A., & Fédèle, E. (2013). Analysis of directional effects on atmospheric correction. *Remote Sensing of Environment*, *128*, 276–288. https://doi.org/10.1016/j.rse.2012.10.018

Franch, Belen, San Bautista, A., Fita, D., Rubio, C., Tarrazó-Serrano, D., Sánchez, A., … Uris, A. (2021). Within-field rice yield estimation based on sentinel-2 satellite data. *Remote Sensing*, *13*(20). https://doi.org/10.3390/rs13204095

Ghimire, B., Rogan, J., & Miller, J. (2010). Contextual land-cover classification: Incorporating spatial dependence in land-cover classification models using random forests and the Getis statistic. *Remote Sensing Letters*, *1*(1), 45–54. https://doi.org/10.1080/01431160903252327

Lisenko, S. A. (2018). Atmospheric correction of multispectral satellite images based on the solar radiation transfer approximation model. *Atmospheric and Oceanic Optics*, *31*(1), 72–85. https://doi.org/10.1134/S1024856018010116

Muchsin, F., Dirghayu, D., Prasasti, I., Rahayu, M. I., Fibriawati, L., Pradono, K. A., … Mahatmanto, B. (2019). Comparison of atmospheric correction models: FLAASH and 6S code and their impact on vegetation indices (case study: Paddy field in Subang District, West Java). *IOP Conference Series: Earth and Environmental Science*, *280*(1). https://doi.org/10.1088/1755-1315/280/1/012034

Muchsin, F., Supriyatna, Harmoko, A., & Prasasti, I. (2022). Evaluation of

Atmospheric Correction Methods of Sentinel-2 for Monitoring Paddy Rice Growth in Cianjur and Klaten Regency. *Journal of Physics: Conference Series*, *2243*(1). https://doi.org/10.1088/1742-6596/2243/1/012023

Muchsin, Fadila, Fibriawati, L., & Pradhono, K. A. (2018). Atmospheric Correction Models of Landsat-7 Imagery. *Jurnal Penginderaan Jauh Dan Pengolahan Data Citra Digital*, *14*(2). https://doi.org/10.30536/j.pjpdcd.1017.v14.a2595

Sola, I., García-Martín, A., Sandonís-Pozo, L., Álvarez-Mozos, J., Pérez-Cabello, F., González-Audícana, M., & Montorio Llovería, R. (2018). Assessment of atmospheric correction methods for Sentinel-2 images in Mediterranean landscapes. *International Journal of Applied Earth Observation and Geoinformation*, *73*(May), 63–76. https://doi.org/10.1016/j.jag.2018.05.020

Ulfa, K., Hendayani, Oktavia, M. I., Pradono, K. A., Fibriawati, L., Muchsin, F., … Damanik, K. W. V. (2020). Evaluation of atmospheric correction algorithms for Sentinel-2 over paddy field area. *IOP Conference Series: Earth and Environmental Science*, *500*(1). https://doi.org/10.1088/1755-1315/500/1/012081

USGS. (2022). *Landsat 8-9 Level 2 Science Product (L2SP) Guide March 2022 Landsat 8-9* (Vol. 2).

Vermote, E. F., & Kotchenova, S. (2008). Atmospheric correction for the monitoring of land surfaces. *Journal of Geophysical Research Atmospheres*, *113*(23), 1–12. https://doi.org/10.1029/2007JD009662